Fluorescence Imaging Enabled Biodegradable Photostable Polymeric Micelles

*Dipendra Gyawali, Shengyuan Zhou, Richard T. Tran, Yi Zhang, Chao Liu, Xiaochun Bai, and Jian Yang**

Amphiphilic diblock or triblock copolymers that are capable of self-assembling into thermodynamically stable nanostructures with a hydrophobic core and hydrophilic corona, referred to as micelles, have become increasingly important in pharmaceutical applications.[1–5] The hydrophobic core can house hydrophobic drugs[6] and the hydrophilic corona functions as a steric barrier to prevent micelle aggregation ensuring micelle solubility in an aqueous environment.[7] To date, multiple synthetic amphiphilic micelle systems (Genexol-PM,[8,9] NK012,[10] SP1049C,[11,12] NC-6004,[13] and NK105)[14,15] are under clinical evaluation for delivering hydrophobic anticancer drugs. The size of these micelles typically range from 10 to 100 nm in diameter, and are composed of a hydrophilic corona, which prevents opsonization resulting in relatively long plasma retention times and reduced uptake by the reticuloendothelial system.[16] The small size of these micelles allows them to accumulate in tumors through an enhanced permeability and retention effect via the leaky microvasculature of tumors, which are characterized by fenestration cutoffs or large gaps ranging from 380 nm up to 1.2 μm.

In recent years, fluorescent micelles have gained significant attention at the forefront of theranostic (therapeutic + diagnostic) nanomedicine.[4,17,18] For example, fluorescent micelles have been used as *in vivo* tracers for cancer detection[19,20] and as probes for investigating the cellular internalization and intracellular trafficking of particles, drugs, and genes.[21] The existing strategies to confer fluorescent properties to micelles are centered on conjugating or encapsulating fluorescent organic dyes (rhodamine, Cyanines, and fluorescein),[22–25] quantum dots (QDs),[26] or gold particles[27,28] on or within the micelles. However, conjugation or encapsulation of these materials is often associated with low dye-to-micelle ratios, increased particle sizes, inferior photobleaching-resistance (organic dyes), and significant cytotoxicity (QDs and other metallic particles), which are inevitable concerns for these fluorescent micelle systems.[29] Furthermore, premature leakage of the dye molecules into surrounding tissues may interfere with the detection of samples of interest.[30]

Recently, our group has made progress in the development of biodegradable photoluminescent polymers (BPLPs), which present intriguing fluorescent properties without the conjugation of any organic dyes or QDs.[31] BPLPs display superior biocompatibility both in vitro and in vivo, high quantum yields (QYs) (up to 79%), photobleaching resistance, and tunable emission up to near infrared wavelengths. The monomers used in the synthesis of BPLPs, citric acid (a metabolite in the Krebs cycle), polyethylene glycol (PEG), aliphatic diols, and all 20 α-amino acids, are all compounds used in many Food and Drug Administration-regulated devices.[31,32] The use of different α-amino acids results in photostable BPLPs with tunable fluorescence properties in terms of their fluorescent intensity, excitation, emission, QY, and so on. BPLPs are referred to as BPLP-Cys and BPLP-Ser when L-cysteine and L-serine are used in the syntheses, respectively. One noteworthy advantage of BPLPs over the traditional organic dyes or QDs is that BPLPs are implantable polymers, and can be fabricated into medical devices, such as nanoparticles and cellular scaffolds, while also functioning as imaging probes. In contrast, organic dyes and QDs are solely imaging probes, which have to be ancillary to other materials and devices.

Given the growing needs for theranostic micelle systems, we describe the synthesis and characterization of photostable fluorescent amphiphilic copolymers based on BPLPs, referred to as amphiphilic BPLPs (ABPLPs) (**Figure 1**A). Supporting information, Scheme S1 shows the synthesis schematic of ABPLPs. BPLPs were used as the hydrophobic block and methoxy poly(ethylene glycol) (MPEG) (MW 750, 2000, and 5000) was used as the hydrophilic block due to its broad acceptance in many micelle systems.[33–35] In step 1, MPEG was first converted to MPEG-COOH by reacting with succinic anhydride. Characteristic bond vibrations illustrated in Fourier transform infrared spectra (Figure S1, Supporting Information) and chemical shifts observed in ^{1}H-NMR spectrum (Figures S2A,B, Supporting Information) confirmed the successful modification of MPEG to MPEG-COOH.

In step 2, the hydrophobic blocks were synthesized similar to the procedures reported in our previous publication.[31] Citric acid was reacted with poly(propylene glycol) (PPG) to form a polyester backbone and further condensed with L-cysteine via

D. Gyawali, S. Zhou, Dr. Y. Zhang
Department of Bioengineering
The University of Texas at Arlington
Arlington, TX 76010, USA
Dr. R. T. Tran, Dr. C. Liu, Prof. J. Yang
Department of Bioengineering
Materials Research Institute
Huck Institutes of The Life Sciences
The Pennsylvania State University
University Park, PA 16802, USA
E-mail: jxy30@psu.edu
Dr. X. Bai
Academy of Orthopedics
Guangdong Province
The Third Affiliated Hospital
Southern Medical University
Guangzhou 510280, China

DOI: 10.1002/adhm.201300145

© 2013 WILEY-VCH Verlag GmbH & Co. KGaA, Weinheim

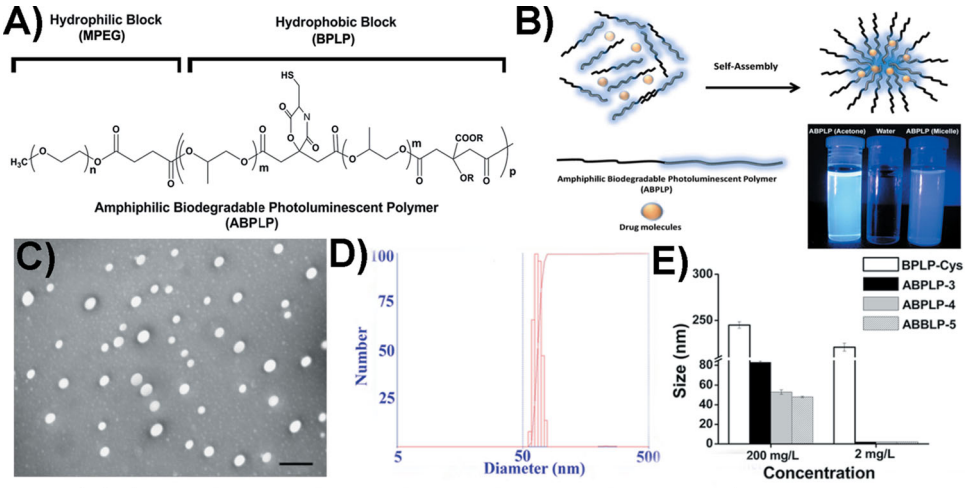

F)

Polymer	PPG/MPEG	CMC (mg/mL)	Size (nm)	Polydispersity	Zeta Potential (mV)
ABPLP-1	425/750	0.01	178±3.50	0.20±0.05	-23.57±2.30
ABPLP-2	725/750	0.006	107±1.10	0.21±0.06	-21.81±1.86
ABPLP-3	2000/750	0.004	68±0.80	0.18±0.03	-27.07±3.00
ABPLP-4	2000/2000	0.005	53±0.70	0.17±0.02	-23.87±2.22
ABPLP-5	2000/5000	0.01	48±0.60	0.16±0.02	-23.77±1.28

Figure 1. Syntheses and characterization of ABPLP particles. A) Chemical structure of ABPLP polymer chain. B) ABPLP copolymers composed of fluorescent hydrophobic blocks can self assemble into core–shell (micelle) structures encapsulating hydrophobic drugs within their core in an aqueous solution. Camera photograph of ABPLP-3 solution (in acetone) and ABPLP micelle (in water) taken under ultraviolet lamp demonstrating their bright fluorescence. C) Representative transmission electron microscopy (TEM) image of ABPLP-3 micelles in aqueous solution. D) Sizes of ABPLP-3 micelles measured by dynamic light scattering. E) Size comparison of ABPLP micelles with BPLP nanoparticles at concentration below (2 mg L^{-1}) and above (200 mgL^{-1}) critical micelle concentration (CMC). F) Summary of composition and particle properties of ABPLP.

the pendent carboxyl group and germinal hydroxyl group of the citrate units to create a six-membered ring. The six-membered planar rings pendant on the BPLP polymer backbones are composed of amide and ester bonds with different R groups from the various amino acids, which is believed to cause the polymer fluorescence through the hyperconjugation theory.[31] The R groups pendant to the α-C in the amino acids likely influence the degree of hyperconjugation, propensity for cyclization, and provide slight perturbations in the associated energy levels resulting in the different emission maxima and QYs observed for the BPLP-amino acids.

In step 3, the –COOH terminal hydrophilic MPEG chains were conjugated with the –OH terminal hydrophobic BPLP chains through DCC/DMAP chemistry to form ABPLPs. Various molecular weights of PPG (425, 725, and 2000 Da) and MPEG (750, 2000, and 5000) were used in the synthesis protocol to understand variation of chain lengths on the properties of ABPLP copolymer.

As amphiphilic copolymers, ABPLPs have the ability to self-assemble into nanosized micelles (Figure 1B,C) in an aqueous medium. ABPLPs can be dissolved in solvents such as acetone, tetrahydrofuran (THF), dimethylformamide, methyl chloride, and dimethylsulfoxide. Under TEM, ABPLP-3 micelles were spherical in shape and 60 nm in diameter, which was in an agreement with the size measurements from dynamic light scattering (an average diameter of 68 nm and a polydispersity index of 0.17) (Figure 1D). No particle aggregation was observed, and ABPLPs synthesized using low molecular weight PPG, as in the case of ABPLP-1 and ABPLP-2, demonstrated higher particle sizes of 178 and 107 nm, respectively. However, ABPLPs synthesized with high molecular weight PPG, as in the case of ABPLP-3, exhibited smaller particle sizes of 68 nm. In addition, particle size can be further reduced with an increase in the hydrophilic block molecular weight as in the case of ABPLP-4 (53 nm) and ABPLP-5 (48 nm).

The thermodynamic stability of micelles can be determined by the CMC. A low CMC is important in maintaining micelle stability and integrity since a major difference between in vitro and in vivo conditions is the effect of dilution after intravenous administration.[36,37] It is well known that the CMC values are mainly dictated by the relative lengths of hydrophobic and hydrophilic blocks. Typically, when the length of the hydrophilic block is held constant, an increase in the length of the hydrophobic blocks results in decreased CMC values.[38] CMC values of 0.012, 0.006, and 0.004 mg mL^{-1} for ABPLP-1, ABLP-2, and ABPLP-3, respectively, in aqueous solution were seen to decrease as the fraction of the PPG hydrophobic block in the amphiphilic copolymers increased (Figure S4, Supporting Information).[39] On the other hand, the CMC values for ABPLP-3, ABPLP-4, and ABPLP-5 were calculated as 0.004, 0.005, and 0.010 mg mL^{-1}, respectively (Figure 1F). When the length of the hydrophobic block remained constant, the CMC

© 2013 WILEY-VCH Verlag GmbH & Co. KGaA, Weinheim

values increased in relation to an increasing hydrophilic block (MPEG) length due to enhanced hydrophilicity.[40] These CMC values are lower than other amphiphilic polymeric micelles reported (1.1 mg mL^{-1} for PEO-b-PHB-b-PEO,[41] 0.07 mg mL^{-1} for PDMAEMA-b-PTHF-b-PDMAEMA, and 0.03 mg mL^{-1} for PDMAEMA-b-PBD-b-PDMAEMA).[42] The lower CMC values for ABPLPs suggest that the ABPLP micelles are potentially more stable after intravenous administration. Based on the "salt out" effect,[43] an even lower CMC value may be expected for micelles in ionic blood solution. To verify the micelle formation, the sizes of ABPLP micelles were measured by DLS at concentrations above and below the CMC for various ABPLP micelles and compared with the nanospheres of BPLPs. Upon dilution below the CMC (0.002 mg mL^{-1}), all the ABPLP micelles completely disassembled and the sizes could not be detected by DLS, whereas BPLP nanospheres displayed stable solid colloidal solutions even at very low concentrations (Figure 1E). In addition, ABPLP micelles displayed a negative zeta potential in deionized water in the range of –20 to –27 mV (Figure 1F), which also contributes to the micelle stability since the strong electrostatic repulsion minimizes micelle aggregation.[44]

ABPLP micelles are a unique biomaterial system due to their unique fluorescent properties inherited from the hydrophobic BPLP blocks.[31] In this study, we primarily investigated the fluorescent properties of a representative ABPLPs, ABPLP-Cys (0.2 molar ratio). As compared with BPLP-Cys, ABPLP-Cys also showed a strong fluorescence emission within the range of 390–550 nm with a peak wavelength at 446 nm (**Figure 2**A). Interestingly, the fluorescent intensity of ABPLP-Cys was significantly reduced in micelle form when compared with that of polymer solution in 1,4-dioxane (Figure 2B). This was further evidenced by the QYs measured for all ABPLP copolymers (Figure 2C,G). For example, the QYs of ABPLP-1, ABPLP-2, ABPLP-3, ABPLP-4, and ABPLP-5 were 0.453, 0.443, 0.447, 0.434, and 0.424, respectively, in a 1,4-dioxane solution. In micelle form, the QYs significantly reduced to 0.046, 0.072, 0.158, 0.256, and 0.266, respectively (Figure 2G). This might be due to the fact that the random chains of amphiphilic block copolymers were fully solvated in the organic solvent system for polymer solutions. In contrast, the fluorescent hydrophobic blocks (fluorophore) of the polymeric chains were drawn together through hydrophobic interactions in micelles, which brings a possibility of fluorescence quenching. This potential fluorescence quenching may contribute to a significant reduction in their QYs. On the other hand, the molar absorption coefficients were found to be significantly higher for all ABPLPs in micelle form when compared with that in 1,4-dioxane solution. This result indicates that ABPLPs have a high capacity for light absorption even though they exhibit relative low QYs when in a micelle form.

The photostability of ABPLP micelles was also investigated and compared with the widely used organic fluorescent dye, rhodamine-B. The fluorescent intensity of the ABPLP micelle solution reduced by only 1% of the initial intensity after continuous UV excitation for 3 h, which indicates excellent photostability (Figure 2D) where as rhodamine-B lost almost 10% of initial fluorescent intensity within the same experimental period. Furthermore, a family of ABPLP polymers was synthesized using different alpha-amino acids. For example,

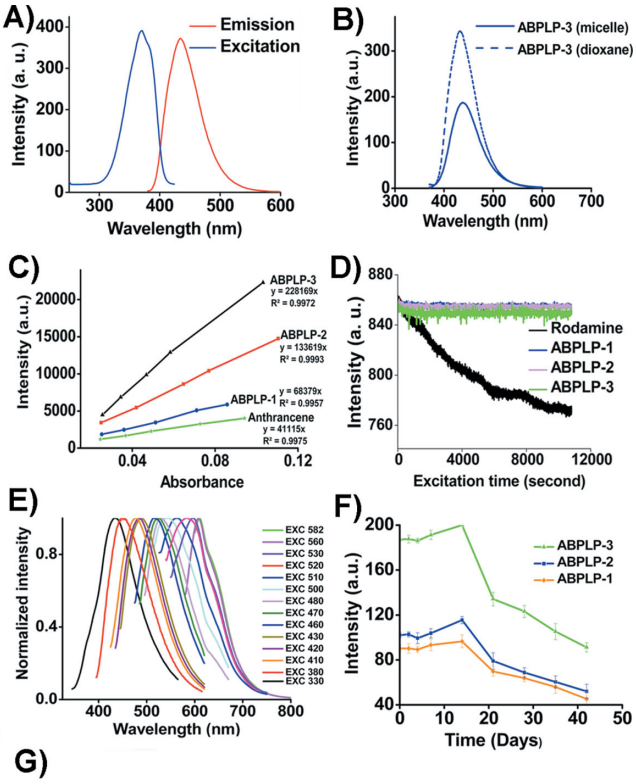

G)

Polymer	QY (Dioxane solution)	QY (Micelle solution)	ε, $L \cdot mol^{-1} \cdot cm^{-1}$ (Dioxane solution)	ε, $L \cdot mol^{-1} \cdot cm^{-1}$ (Micelle solution)
ABPLP-1	0.453	0.047	514.5	5560
ABPLP-2	0.443	0.072	345.9	3560
ABPLP-3	0.447	0.158	360	2450
ABPLP-4	0.434	0.256	342.4	1810
ABPLP-5	0.424	0.266	356.8	1740

Figure 2. Photoluminescent properties of ABPLPs. A) Excitation and emission spectra of ABPLP- 3 micelles in water. B) Emission spectra of ABPLP solution in 1,4-dioxane and ABPLP micelles in water excited at 350 nm. C) Intensity–absorbance curve of ABPLP-1, ABPLP-2, and ABPLP-3 for QY measurements. D) Photostability evaluation of ABPLP-1, ABPLP-2, and ABPLP-3 and control organic dye rhodamine, E) emission spectra of ABPLP-Ser, and F) fluorecent intensity of ABPLP-1, ABPLP-2, and ABPLP-3 at various time periods when incubated in phosphate buffer solution (pH 7.4). G) Summary of fluorescent properties of ABPLP micelles (ε: molar absorption coefficient).

ABPLP-Ser, when synthesized with L-serine, exhibits different fluorescent colors ranging from blue to red by varying the excitation wavelength (Figure 2E) similar to BPLP-Ser. The excitation-dependent emission of ABPLP-Ser was ascribed to a well-known Red-Edge Effect where polar and rotatable fluorophores embedded in rigid and highly viscous medium can generate variable fluorescence emission.[45,46] In our BPLP or ABPLP structure, the polymer backbones can be treated as a viscous medium for the pendent six-membered ring fluorophores. The R group (–CH_2OH) on the six-membered ring of ABPLP-Ser is highly rotatable, which allows ABPLP-Ser to display excitation dependence. However, we have previously demonstrated that an easy H_2S elimination occurs during the BPLP-Cys or ABPLP-Cys formation, which results in a double bond formation to extend the conjugation system of the six-membered ring

© 2013 WILEY-VCH Verlag GmbH & Co. KGaA, Weinheim

(Figure S5, Supporting Information). The double bond may restrict the rotation of the fluorophore. Therefore, ABPLP-Cys does not show excitation dependence for its emission.

Finally, the long-term fluorescent stability of ABPLP micelles in an aqueous system was monitored for a 6-week period (Figure 2F). In the first week, the fluorescent intensity of the micelles was nearly constant for all micelle systems, followed by an increase in the fluorescent intensity at 2 weeks, and then a continuous decrease thereafter. This result strongly suggests that ABPLP micelles maintained their thermodynamic stability in the first week and then displayed a higher fluorescent intensity due to dissociation of the polymeric chains after week 2. The continuous decrease in fluorescent intensity afterwards was due to the degradation of the BPLP chains of ABPLPs, which is also in agreement with the degradation profile of fluorescent blocks of the previously published BPLPs.[31]

To demonstrate the potential of ABPLP micelles for imaging applications, the cellular uptake and fluorescent imaging of the micelles both in vitro and in vivo were conducted. ABPLP micelles were used to label NIH 3T3 fibroblasts with fluorescence colors after 3 h of incubation (**Figure 3**A,B). The micelles may have only accumulated on the cell surfaces at 3 h thus the entire cell bodies seem fluorescent. When cells were imaged at 9 h, cell nuclei were obvious and the cytoplasm was labeled with a blue color suggesting the micelles were uptaken by the cells. When incubated with NIH 3T3 fibroblasts for 24 h, ABPLP micelles did not show significant cytotoxicity to the cells at concentrations ranging from 1 to 1000 μg mL^{-1}. It was also noted that ABPLPs with smaller micelle size (as in the case of ABPLP-3, ABPLP-4, and ABPLP-5) were noncytotoxic even at high concentrations (>500 μg mL^{-1}) (Figure 3C). To verify the potential for in vivo imaging, ABPLP micelle solutions of various concentrations were subcutaneously injected in a mouse through a 27-gauge needle. ABPLP micelles were detected using a noninvasive in vivo imaging system. As illustrated in Figure 3D, the signal intensity doubled when the concentration was increased from 0.0625 to 1 mg mL^{-1}. Upon closer topical observation of the surrounding tissue at the injection sites, the ABPLP micelles did not induce redness or obvious irritation. These in vitro and in vivo studies suggest that ABPLP micelle systems possess great potential for in vitro cell labeling and in vivo tissue imaging.

To demonstrate the utility of ABPLP micelles for cancer drug delivery,[47,48] Paclitaxel (PTX) was used as a model cancer drug for in vitro drug delivery and cell culture studies.[49] It was observed that all ABPLP micelles have high drug (PTX) loading and encapsulation efficiencies of 20.6%–22.78% and 81.57%–91.12%, respectively, as shown in Figure S6A (Supporting Information). The PTX release profiles from various ABPLP micelles (Figure S6B, Supporting Information) showed an initial burst release (≈50% of the initial loading amount) in the first stage up to 10 h followed by a sustained release period of up to 96 h as similar to other micelle drug delivery systems.[50,51] When incubated with a human prostrate cancer cell line (PC-3) (Figure S6C, Supporting Information), no sign of cellular toxicity was observed for cells incubated with media containing 0.5 mg mL^{-1} of drug-free micelles. However, PTX-loaded ABPLP micelles resulted in delayed cell toxicity with the final toxicity at 24 h comparable to free PTX. These results support that ABPLP micelles may potentially serve as a viable cancer drug carrier to release a significant amount of drugs after reaching the targeting sites through the circulation in vivo.

In this work, we reported photobleaching resistant ABPLPs that can be self-assembled into fluorescent micelles. ABPLP micelles could label NIH 3T3 fibroblasts without inducing significant cellular toxicity. PTX-loaded ABPLP micelles could delay the release of payload to kill prostrate cancer PC3 cells. In vivo imaging studies showed that ABPLP micelles emitted strong fluorescence in vivo when injected subcutaneously. It is the first time to report biodegradable amphiphilic photoluminescent polymers without conjugating any conventional fluorescent

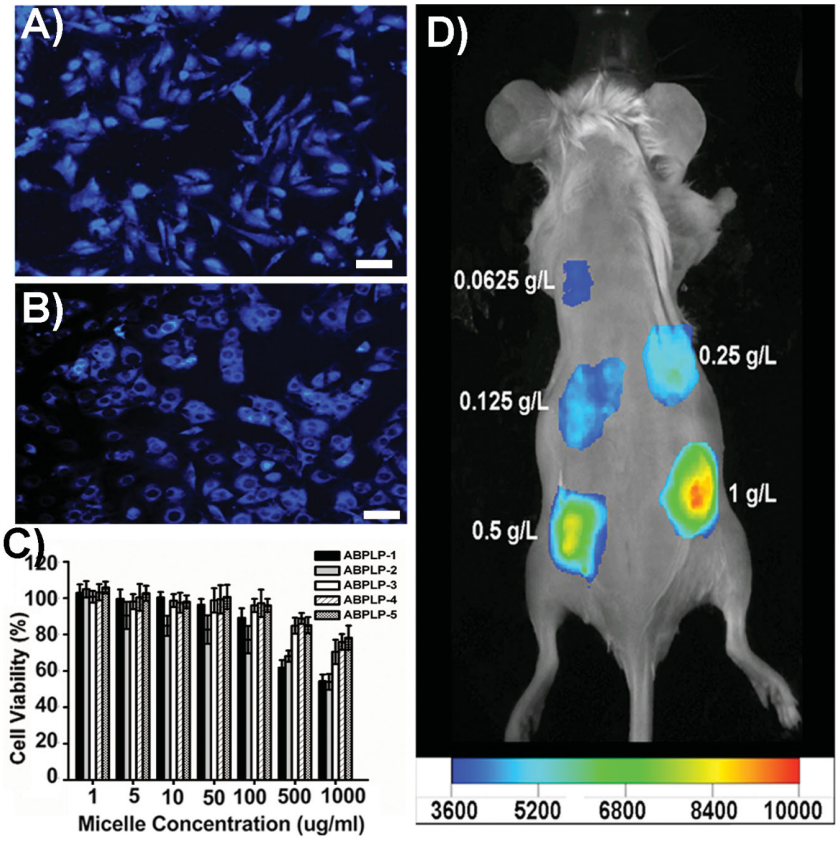

Figure 3. In vitro cellular uptake and in vivo fluorescence imaging of ABPLP micelles. ABPLP-3 micelle-uptaken 3T3 fibroblasts observed under fluorescent microscope with DAPI filter (4×) at A) 3 h and B) 9 h. C) Cytotoxicity evaluation (MTT assay) of ABPLP micelles against 3T3 fibroblast at various concentrations (1–1000 μg mL^{-1}). Values were normalized to the viability of cells cultured in micelle-free medium. D) Fluorescence image of ABPLP micelles injected in a nude mouse at various concentrations (0.0625–1 g L^{-1}).

© 2013 WILEY-VCH Verlag GmbH & Co. KGaA, Weinheim

organic dyes or QDs. ABPLP micelles may serve as an ideal vector in theranostic nanomedicine.

Experimental Section

The detailed experimental procedures are available in the Supporting Information.

Supporting Information

Supporting Information is available from the Wiley Online Library or from the author.

Acknowledgements

This work was supported in part by a NSF CAREER award (DMR 1313553), a NIBIB R01 award (EB012575), a CPRIT High Impact/High Risk Research Award (RP110412), and a research award from National Natural Sciences Foundation of China (31228007).

Received: April 19, 2013
Revised: May 14, 2013
Published online: August 26, 2013

[1] Y. Matsumura, *Adv. Drug Delivery Rev.* **2008**, *60*, 899.
[2] A. Rosler, G. W. M. Vandermeulen, H. A. Klok, *Adv. Drug Delivery Rev.* **2001**, *53*, 95.
[3] Z. L. Tyrrell, Y. Q. Shen, M. Radosz, *Prog. Polym. Sci.* **2010**, *35*, 1128.
[4] C. Oerlemans, W. Bult, M. Bos, G. Storm, J. F. W. Nijsen, W. E. Hennink, *Pharm. Res.* **2010**, *27*, 2569.
[5] X. R. Li, Z. L. Yang, K. W. Yang, Y. X. Zhou, X. W. Chen, Y. H. Zhang, F. Wang, Y. Liu, L. J. Ren, *Nanoscale Res. Lett.* **2009**, *4*, 1502.
[6] V. P. Torchilin, *Pharm. Res.* **2007**, *24*, 1.
[7] M. C. Jones, J. C. Leroux, *Eur. J. Pharm. Biopharm.* **1999**, *48*, 101.
[8] T. Y. Kim, D. W. Kim, J. Y. Chung, S. G. Shin, S. C. Kim, D. S. Heo, N. K. Kim, Y. J. Bang, *Clin. Cancer Res.* **2004**, *10*, 3708.
[9] K. S. Lee, H. C. Chung, S. A. Im, Y. H. Park, C. S. Kim, S. B. Kim, S. Y. Rha, M. Y. Lee, J. Ro, *Breast Cancer Res. Treat.* **2008**, *108*, 241.
[10] Y. Matsumura, K. Kataoka, *Cancer Sci.* **2009**, *100*, 572.
[11] J. W. Valle, A. Armstrong, C. Newman, V. Alakhov, G. Pietrzynski, J. Brewer, S. Campbell, P. Corrie, E. K. Rowinsky, M. Ranson, *Invest. New Drugs* **2011**, *29*, 1029.
[12] J. W. Valle, J. Lawrance, J. Brewer, A. Clayton, P. Corrie, V. Alakhov, M. Ranson, *J. Clin. Oncol.* **2004**, *22*, 362s.
[13] R. Plummer, R. H. Wilson, H. Calvert, A. V. Boddy, M. Griffin, J. Sludden, M. J. Tilby, M. Eatock, D. G. Pearson, C. J. Ottley, Y. Matsumura, K. Kataoka, T. Nishiya, *Br. J. Cancer* **2011**, *104*, 593.
[14] K. Kato, T. Hamaguchi, H. Yasui, T. Okusaka, H. Ueno, M. Ikeda, K. Shirao, Y. Shimada, H. Nakahama, K. Muro, Y. Matsumura, *J. Clin. Oncol.* **2006**, *24*, 83s.
[15] T. Hamaguchi, K. Kato, H. Yasui, C. Morizane, M. Ikeda, H. Ueno, K. Muro, Y. Yamada, T. Okusaka, K. Shirao, Y. Shimada, H. Nakahama, Y. Matsumura, *J. Cancer* **2007**, *97*, 170.
[16] V. P. Torchilin, *Pharm. Res.* **2007**, *24*, 1.
[17] C. Khemtong, C. Kessinger, J. M. Gao, *Chem. Commun.* **2009**, 3497.
[18] J. H. Park, G. von Maltzahn, L. L. Ong, A. Centrone, T. A. Hatton, E. Ruoslahti, S. N. Bhatia, M. J. Sailor, *Adv. Mater.* **2010**, *22*, 880.
[19] N. Nasongkla, E. Bey, J. M. Ren, H. Ai, C. Khemtong, J. S. Guthi, S. F. Chin, A. D. Sherry, D. A. Boothman, J. M. Gao, *Nano Lett.* **2006**, *6*, 2427.
[20] B. Sumer, J. M. Gao, *Nanomedicine* **2008**, *3*, 137.
[21] J. Lu, S. C. Owen, M. S. Shoichet, *Macromolecules* **2011**, *44*, 6002.
[22] L. B. Luo, J. Tam, D. Maysinger, A. Eisenberg, *Bioconjug. Chem.* **2002**, *13*, 1259.
[23] I. Texier, M. Goutayer, A. Da Silva, L. Guyon, N. Djaker, V. Josserand, E. Neumann, J. Bibette, F. Vinet, *J. Biomed. Opt.* **2009**, 14.
[24] D. Q. Wu, B. Lu, C. Chang, C. S. Chen, T. Wang, Y. Y. Zhang, S. X. Cheng, X. J. Jiang, X. Z. Zhang, R. X. Zhuo, *Biomaterials.* **2009**, *30*, 1363.
[25] H. I. Lee, W. Wu, J. K. Oh, L. Mueller, G. Sherwood, L. Peteanu, T. Kowalewski, K. Matyjaszewski, *Angew. Chem. Int. Ed.* **2007**, *46*, 2453.
[26] J. Lee, J. H. Im, K. M. Huh, Y. Lee, H. Shin, *J. Nanosci. Nanotechnol.* **2010**, *10*, 487.
[27] T. Sakai, P. Alexandridis, *Langmuir* **2004**, *20*, 8426.
[28] H. Otsuka, Y. Akiyama, Y. Nagasaki, K. Kataoka, *J. Am. Chem. Soc.* **2001**, *123*, 8226.
[29] A. V. Kabanov, V. I. Slepnev, L. E. Kuznetsova, E. V. Batrakova, V. Y. Alakhov, N. S. Meliknubarov, P. G. Sveshnikov, V. A. Kabanov, *Biochem. Int.* **1992**, *26*, 1035.
[30] J. X. Zhang, L. Y. Qiu, X. D. Li, Y. Jin, K. J. Zhu, *Small* **2007**, *3*, 2081.
[31] J. Yang, Y. Zhang, S. Gautam, L. Liu, J. Dey, W. Chen, R. P. Mason, C. A. Serrano, K. A. Schug, L. Tang, *Proc. Natl. Acad. Sci. U.S.A.* **2009**, *106*, 10086.
[32] A. S. Wadajkar, T. Kadapure, Y. Zhang, W. Cui, K. T. Nquyen, M. Samchukov, J. Yang, *Adv. Healthcare Mater.* **2012**, *1*, 450.
[33] G. Gaucher, M. H. Dufresne, V. P. Sant, N. Kang, D. Maysinger, J. C. Leroux, *J. Controlled Release* **2005**, *109*, 169.
[34] E. Allemann, N. Brasseur, O. Benrezzak, J. Rousseau, S. V. Kudrevich, R. W. Boyle, J. C. Leroux, R. Gurny, J. E. Vanlier, *J. Pharm. Pharmacol.* **1995**, *47*, 382.
[35] G. H. Gao, J. W. Lee, M. K. Nguyen, G. H. Im, J. Yang, H. Heo, P. Jeon, T. G. Park, J. H. Lee, D. S. Lee, *J. Controlled Release* **2010**, *123*, 109.
[36] N. Fairley, B. Hoang, C. Allen, *Biomacromolecules* **2008**, *9*, 2283.
[37] R. Savic, A. Eisenberg, D. Maysinger, *J. Drug Target.* **2006**, *14*, 343.
[38] S. K. Varshney, X. F. Zhong, A. Eisenberg, *Macromolecules* **1993**, *26*, 701.
[39] R. Nagarajan, K. Ganesh, *Macromolecules* **1989**, *22*, 4312.
[40] D. Wang, Z. P. Peng, X. X. Liu, Z. Tong, C. Y. Wang, B. Ren, *Eur. Polym. J.* **2007**, *43*, 2799.
[41] J. Li, X. P. Ni, X. Li, N. K. Tan, C. T. Lim, S. Ramakrishna, K. W. Leong, *Langmuir* **2005**, *21*, 8681.
[42] M. Even, D. M. Haddleton, D. Kukulj, *Eur. Polym. J.* **2003**, *39*, 633.
[43] A. Patist, J. R. Kanicky, P. K. Shukla, D. O. Shah, *J. Colloid Interface Sci.* **2002**, *245*, 1.
[44] N. Kallay, S. Zalac, *J. Colloid Interface Sci.* **2002**, *253*, 70.
[45] A. P. Demchenko, *Luminescence* **2002**, *17*, 19.
[46] A. N. Fletcher. *J. Phys. Chem.* **1968**, *72*, 2742.
[47] Y. H. Tao, R. Liu, M. Q. Chen, C. Yang, X. Y. Liu, *J. Mater. Chem.* **2012**, *22*, 373.
[48] H. J. Liang, Q. X. Yang, L. Deng, J. Z. Lu, J. M. Chen, *Drug Dev. Ind. Pharm.* **2011**, *37*, 597.
[49] J. Liu, H. Lee, C. Allen, *Curr. Pharm. Des.* **2006**, *12*, 4685.
[50] E. Blanco, E. A. Bey, Y. Dong, B. D. Weinberg, D. M. Sutton, D. A. Boothman, J. Gao, *J. Controlled Release* **2007**, *122*, 365.
[51] H. Liu, S. Farrell, K. Uhrich, *J. Controlled Release* **2000**, *68*, 167.
[52] M. Licciardi, G. Cavallaro, M. Di Stefano, G. Pitarresi, C. Fiorica, G. Giammona, *Int. J. Pharm.* **2010**, *396*, 219.

© 2013 WILEY-VCH Verlag GmbH & Co. KGaA, Weinheim

Copyright WILEY-VCH Verlag GmbH & Co. KGaA, 69469 Weinheim, Germany, 2014.

ADVANCED HEALTHCARE MATERIALS

Supporting Information

for *Adv. Healthcare Mater.*, DOI: 10.1002/adhm.201300145

Fluorescence Imaging Enabled Biodegradable Photostable Polymeric Micelles

*Dipendra Gyawali, Shengyuan Zhou, Richard T. Tran, Yi Zhang, Chao Liu, Xiaochun Bai, and Jian Yang**

Submitted to ADVANCED HEALTHCARE MATERIALS

Supporting Information

Fluorescence Imaging Enabled Biodegradable Photostable Polymeric Micelles

By *Dipendra Gyawali*, *Shengyuan Zhou*, *Richard T. Tran*, *Yi Zhang*, *Chao Liu*, *Xiaochun Bai* and *Jian Yang**

Experimental Section

Polymer synthesis and characterization: Carboxylic acid-terminated methoxy poly(ethylene glycol) (MPEG-COOH) was prepared via an esterification process (**Figure 1**). Briefly, MPEG (20 mmol) was dissolved with anhydrous toluene (200 mL) in a 500 mL round bottom flask. Succinic anhydride (40 mmol) was added, and the reaction mixture was refluxed at 150 °C for 10 h. After the solution cooled, the residue was filtered out, and the remaining toluene was distilled under reduced pressure. Next, the polymer was dissolved in hot water (20 ml, 70 ºC). The collected organic phase was then dried with anhydrous Na_2SO_4, stirred overnight, filtered, and distilled under vacuum. Dry ethyl ether (20 ml) was then added drop wise into the $CHCl_3$ polymer solution (3 ml), and the top layer of ethyl ether was discarded. This extraction process was repeated three times, and the collected organic phase was finally dried under vacuum. In order to study the effect of the hydrophilic segment size on the resulting micelle properties, PPGs of various molecular weights (750, 2000, and 5000 Da) were used.

In the next step, BPLP was synthesized as previously reported [31] except with a few modifications. Briefly, PPG, citric acid, and L-cysteine with molar ratios of 1.1:1.0:0.2, respectively, were added to a 100 mL round bottom flask, and melted by continuous stirring at 160 ºC. After melting the mixture, the temperature of the system was lowered to 140 ºC, and allowed to condense for 4 hours. Next, the polymer was dissolved in 1,4-dioxane, and precipitated by drop-wise addition into deionized water under constant stirring. Finally, the purified BPLP was collected and dried using lyophilization. In order to study the effect of the hydrophobic segment size on the resulting micelle properties, PPG of various molecular weights (425, 725, and 2000 Da) were used.

Finally, conjugation of hydrophobic BPLP segment and hydrophilic MPEG segment was performed by DMAP/DCC chemistry. Briefly, BPLP (2.5 mmol), MPEG-COOH (2.5 mmol), N-dimethyl aminopyridine (DMAP) (0.5 mmol), and dicyclohexyl carbodiimide (DCC) (10 mmol) were added to a 100 mL round bottom flask containing 1,4-dioxane at room (10 ml) temperature while stirring and maintained for 24 h. After 24 h, the precipitated dicyclohexylurea (DCU) was filtered out and the filtrate was concentrated under reduced pressure and quickly poured into a large amount of cold diethyl ether with vigorous stirring. After filtering under reduced pressure, the product was further placed in a dialysis bag (molecular weight cut-off 2 kDa) to remove any unreacted segments. After 72h of dialysis, the purified product was collected via lyophilization.

Characteristic bond vibrations and chemical shifts of the various protons associated with respective structures of all the three segments (hydrophilic, hydrophobic, and amphiphilic) were analyzed using Nicolet 6700 Fourier Transform Infrared (FTIR) spectrometer (Thermo Fisher Scientific) and 300 MHz JNMECS 300 (JEOL, Tokyo, Japan) respectively. For FTIR analysis, purified polymer was dissolved in acetone to make a 5.0 wt.-% solution. The polymer solution was then cast onto potassium bromide pellets, and the solvent was allowed to evaporate overnight. For ^{1}H-NMR analysis, polymer (5.0 mg) was dissolved in deuterated dimethyl sulfoxide (DMSO-d_6) (1.0 ml). ^{1}H-NMR spectra of proton chemical shifts were collected at room temperature with tetramethylsilane used as internal reference.

Micelle preparation and characterization: To prepare ABPLP micelle solutions, ABPLP (100 mg) was dissolved in acetone (5.0 ml) to make a 2.0% w/v solution. Then, the 2.0% w/v polymeric solution (500 µL) was added drop wise into deionized water (20 mL) under gentle stirring. The acetone was allowed to evaporate at room temperature for several hours to produce an aqueous solution of micelles.

The critical micelle concentration (CMC) of amphiphilic copolymer in aqueous solution was determined by a fluorescence probe technique where pyrene was used as a hydrophobic flourecent probe. The fluorescence spectra of the samples was acquired using a Shimadzu RF-5301 PC fluorospectrophotometer at room temperature. The pyrene-loaded micelle solution was prepared as described elsewhere.[52] Briefly, a known amount of pyrene in acetone was added into 10 mL vials and the acetone was allowed to evaporate. Next, aqueous ABPLP solutions at various concentrations (1×10^{-4} to 10 mg/mL) with the final concentration of pyrene as 6.0×10^{-7} M were prepared for further analysis. Excitation and emission spectra of pyrene were recorded at room temperature and the ratios of the peak intensities at 338 and 333 nm (I_{338}/I_{333}) of the spectra were analyzed as a function of polymer concentration. The CMC value was taken from the intersection of the tangent to the curve at the inflection with the horizontal tangent through the point at the low concentrations.

Hydrodynamic diameter, polydispersity, and surface charge of the ABPLP micelles and BPLP particles was measured at concentration below and above CMC values using a zeta potential analyzer (ZetaPALS, Brookhaven Instruments, Holtsville, NY) equipped with dynamic light scattering (DLS) detector. The morphology of the block copolymer micelles was characterized by transmission electron microscope (TEM, JEOL 1200 EX, Tokyo, Japan). TEM image of the micelles was operated at an acceleration voltage of 80 kV. Samples for TEM observation were prepared by depositing a drop of polymeric micelles onto a mesh copper grid coated with carbon. After the deposition, the aqueous solution was blotted away with a strip of filter paper and allowed to dry. Video files of ABPLP micelles moving under Brownian motion at high (1.0 mg/mL) and low (0.2 mg/mL) concentrations were observed with a NanoSight LM10SH (NanoSight, Amesbury, United Kingdom) equipped with a sample chamber with a 532-nm laser.

Fluorescence studies: Photoluminescent spectra of BPLP and ABPLP polymers and micelle solutions were acquired on a Shimadzu RF-5301 PC fluorospectrophotometer. The optimal excitation wavelength for each type of the micelle solution emission test was determined as the wavelength that generated the highest emission intensity. In this study, BPLPs and ABPLPs were excited at 360 nm, and the excitation and the emission slit widths were both set at 1.5 nm for all samples unless otherwise stated.

The fluorescent quantum yields of the ABPLP in both solvent and in micelle form were measured using the Williams method. The solutions were scanned at optimal excitation wavelength. Then, the UV-vis absorbance spectrum was collected with the same solution and the absorbance at the optimal excitation wavelength was noted. Next, a series of solutions were prepared with gradient concentrations. The absorbance of the each solution was controlled within the range of 0.01–0.1 Abs units. The fluorescence spectrum was also collected for the same solution in the 10 mm fluorescence cuvette. The fluorescence intensity, which is the area of the fluorescence spectrum, was calculated and noted. Polymer solutions with different concentrations were measured and the graphs of integrated fluorescence intensity vs. absorbance were plotted. The quantum yields of the ABPLPs were calculated according to equation (1) where, Φ = quantum yield; slope = gradient of the curve obtained from the plot of intensity versus absorbance; η = refractive index of the solvent; x = subscript to denote the sample, and ST = subscript to denote the standard.

$$\Phi_X = \Phi_{ST}\left(\frac{\text{Slope}_X}{\text{Slope}_{ST}}\right)\left(\frac{\eta_X}{\eta_{SF}}\right)^2 \quad (1)$$

Anthracene (Φ= 0.27 in ethanol) was used as a standard. The ABPLP polymers were dissolved in 1,4-dioxane and anthracene was dissolved in ethanol. The slit width was kept similar for both the standard and samples. Absorbance was measured using a SHIMADZU

UV-2450 spectrophotometer. The molar absorption coefficient (ε, $L \cdot mol^{-1} \cdot cm^{-1}$) of the BPLPs and ABPLPs was calculated according to the Beer-Lambert law, where $A = \varepsilon CL$. All the experiments were carried out in triplicate.

Drug loading and release study: Paclitaxel (PTX) loaded ABPLP micelles were prepared using the solvent evaporation method. In particular, ABPLP (100 mg) polymer in DMF (5 mL) was mixed with PTX (25 mg, a hydrophobic anti-cancer drug used widely in pharmaceutical research). The mixture was stirred for 2 h in a closed container. the polymer/drug solution (500 μL) was added drop wise under gentle stirring to deionized water (20 mL) . Thereafter, the mixture was dialyzed against deionized water using dialysis tubing molecular weight cut-off 500 Da for 24 h. In order to determine the drug loading (DL) and encapsulation efficiency (EE), drug loaded micelles were centrifuged at 12000 rpm. Then, the PTX in the supernatant was assayed by a SHIMADZU UV-2450 spectrophotometer at a wavelength of 227 nm. The DL was defined as percentage of PTX to micelle and EE was defined as the percentage of actual amount of PTX encapsulated to the original amount of PTX.

After dialysis, *in vitro* drug release studies were performed in phosphate buffer saline (100 mL, PBS; pH 7.4) as a releasing medium at 37 °C. PTX-loaded ABPLP micelles (10 mL) was placed in a dialysis bag (Mw cut-off of 500 Da). The dialysis bag was then immersed in the release medium and kept in a horizontal laboratory shaker at a constant temperature (37 °C). In order to measure the drug release content, samples (1 mL) were removed periodically and the fresh PBS replaced an equivalent volume. The amount of released PTX was analyzed with a UV-visible spectrophotometer at 227 nm. Absorbance was measured using a SHIMADZU UV-2450 spectrophotometer. The experiments were performed in triplicate for each of the samples.

Cytotoxicity and bio-imaging studies: The relative cytotoxic effects of ABPLP were evaluated using colorimetric MTS assays (CellTiter 96® AQ_{ueous} One Solution Cell Proliferation Assay, Promega Corp., Madison, WI)) against NIH-3T3 fibroblasts cells according to the manufacture protocol. Briefly, 100 μL of 3T3 mouse fibroblasts (5×10^4 cells/mL) in DMEM supplemental medium, 10% fetal bovine serum, and 1% of penicillin/streptomycin (100 U/mL penicillin and 100 μg/mL streptomycin) were cultured in a 96-well plate (Costar®, Corning Inc., Corning, NY) for 24 h at 37º C, 5% CO_2. The culture medium was then removed and replaced with ABPLP micelles solutions at different concentrations (0–1 mg/mL) in complete DMEM media. After 24 h of incubation, the medium was replaced by fresh media (100 μL) and MTS stock solution (20 μL) . The cultures were incubated for another 4 h, and the absorbance of the dissolved tetrazolium salt solution was measured at 490 nm using a microplate reader. The relative cell viability was calculated by the following equation: relative cell viability (%) = (ODtreated/ODcontrol)×100, where ODcontrol was obtained in the absence of copolymers and ODtreated was obtained in the presence of copolymers. The percentage of relative cell survival to the control (cells exposed to regular culture media) was estimated.

The pharmacological activity of PTX loaded ABPLP micelles was evaluated against PC3 cells using MTS assay as described above. 200 μL of various dilutions of PTX (0.01 to 0.25 mg/mL)-loaded ABPLP-3 micelles were incubated with PC3 cells ($5x10^4$) cultured in a 96-well plate. MTS assay was performed at various time points (4, 12, 24, and 48 h) to understand the pharmacological effect of the drug loaded ABPLP micelles. Drug free ABPLP-3 (0.5 mg/mL) and PTX (0.25 mg/mL) were used as positive and negative controls, respectively. The percentage of relative cell survival to the control (cells exposed to regular culture media) was estimated.

Amphiphilic block copolymer ABPLP-3 was used as representative micelles for cellular imaging studies since it demonstrated the lowest CMC (0.004 mg/mL) compared the other ABPLPs. 3T3 mouse fibroblasts were pre-seeded on sterile glass cover slips at a density of 5,000 cells per mL. After the cells grew to approximately 60% confluency, the cover slip is washed with PBS, transferred to new a petri dish, and incubated with a solution of ABPLP-3 micelles at 0.5 mg/mL. After 3h incubation at 37 °C, the cells were washed by PBS and observed under fluorescence microscope. For longer cell uptake studies (after 3h of incubation of cell with micelle solution), the micelle solution was replace with culture media and incubated for the desired duration and observed under fluorescence microscope.

For micelle *in vivo* bioimaging studies, ABPLP micelle solutions at various concentrations (0.0625 to 1g/L) were sterilized by filtering through a syringe filter (0.22 μm) and injected into C57BL/6 mice, purchased from Taconic Farms (Germantown, NY). After 30 minutes, the mice were imaged using Kodak In-Vivo FX Pro system (Carestream Health Inc., New Haven, CT, USA) with excitation wavelength of 510 nm and emission wavelength of 535 nm. The region of interest was drawn after background correction over the injected site, and the mean fluorescence intensities for all pixels in the flourecent images were calculated using Carestream Molecular Imaging Software, Network Edition 4.5 (Carestream Health). Animals were cared for in compliance with the regulations of the animal care and use committee (IACUC) of The University of Texas at Arlington.

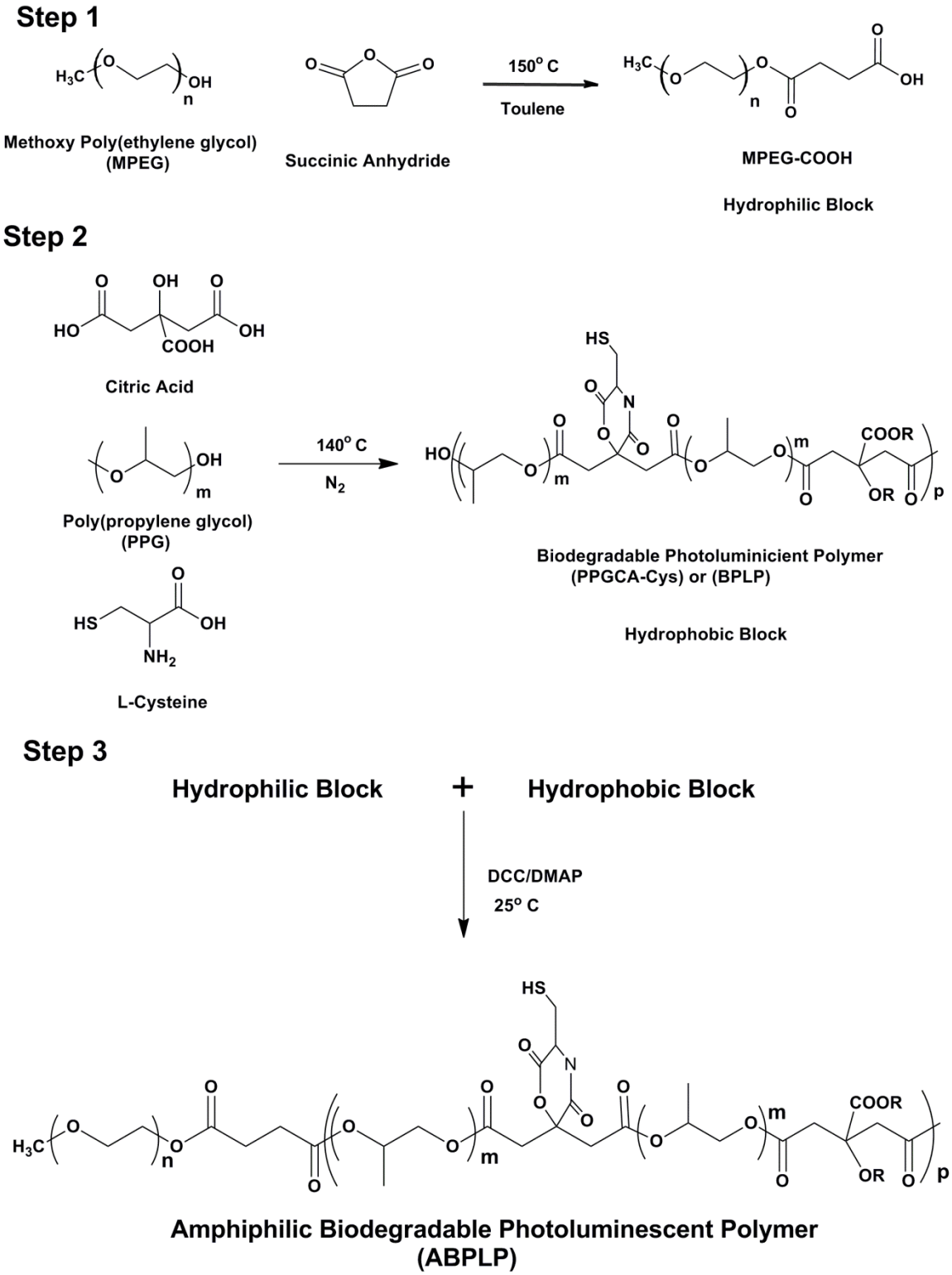

Scheme S1. Schematic representation of amphiphilic biodegradable photoluminescent polymer syntheses. Step 1: MPEG was reacted with succinic anhydride at 150 °C in toluene solvent system to terminate MPEG with carboxylic acid functional group. Step 2: citric acid, poly (propylene glycol) and L-cysteine were polycondensed at 140 °C to create biodegradable photoluminescent polymer. Step 3: carboxylic acid terminated MPEG (Hydrophilic block) of various molecular weight (400, 750, and 2000 Da) was polymerized with hydroxyl terminated BPLP (Hydrophobic block) with various molecular weight of PPG (425, 725, and 2000 Da) into ABPLP (MPEG-b-PPG-cys).

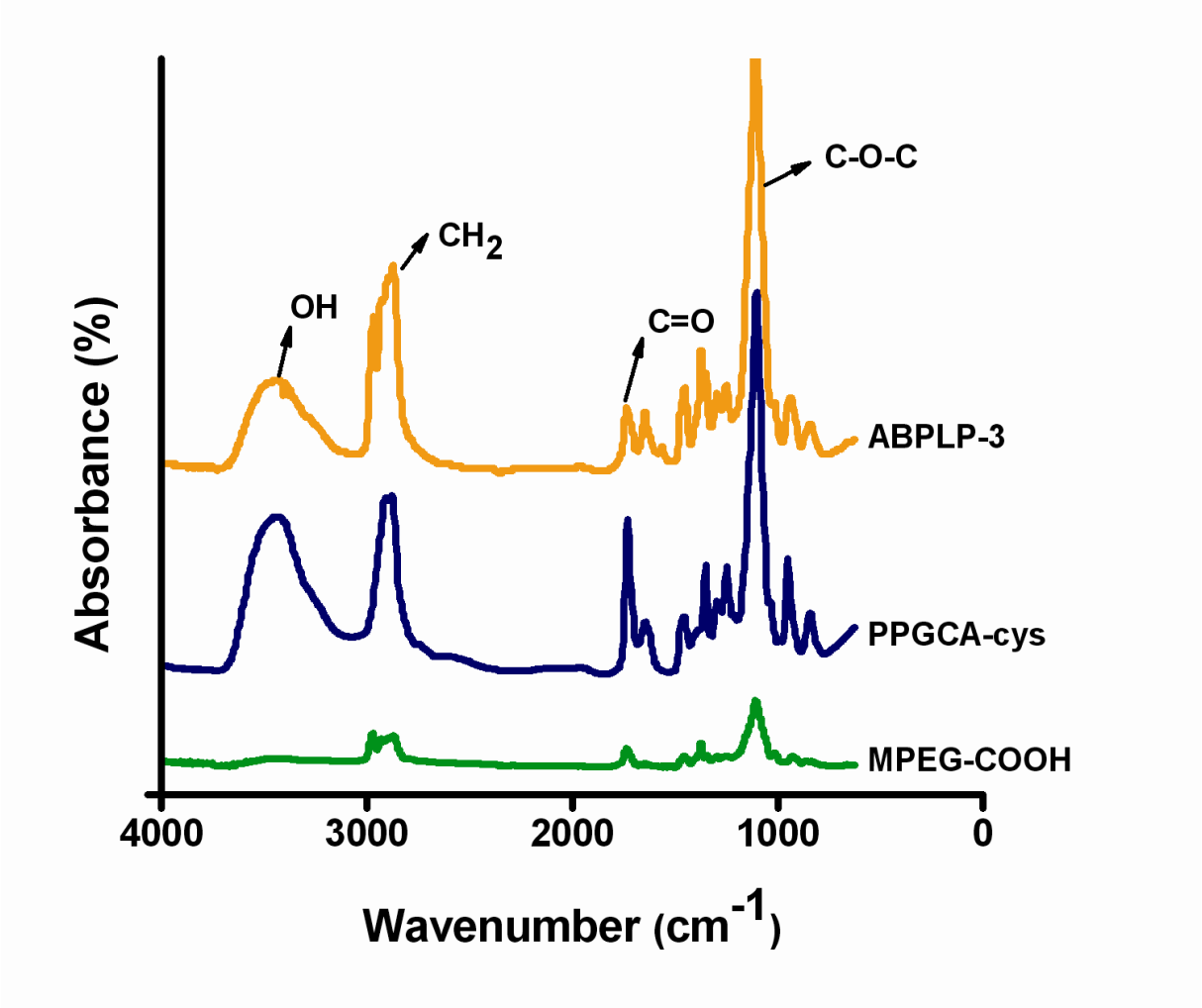

Figure S1. FTIR spectra of hydrophilic block (MPEG-COOH), hydrophobic block (BPLP), and amphiphilic ABPLP. (carbonyl (C=O) peak at 1690–1750 cm^{-1}, hydroxyl (OH) peak 3400 cm^{-1} from succinic acid, methylene (CH_2) peak at 2877 cm^{-1}, and ether (C–O–C) peak at 1112 cm^{-1} from PEG).

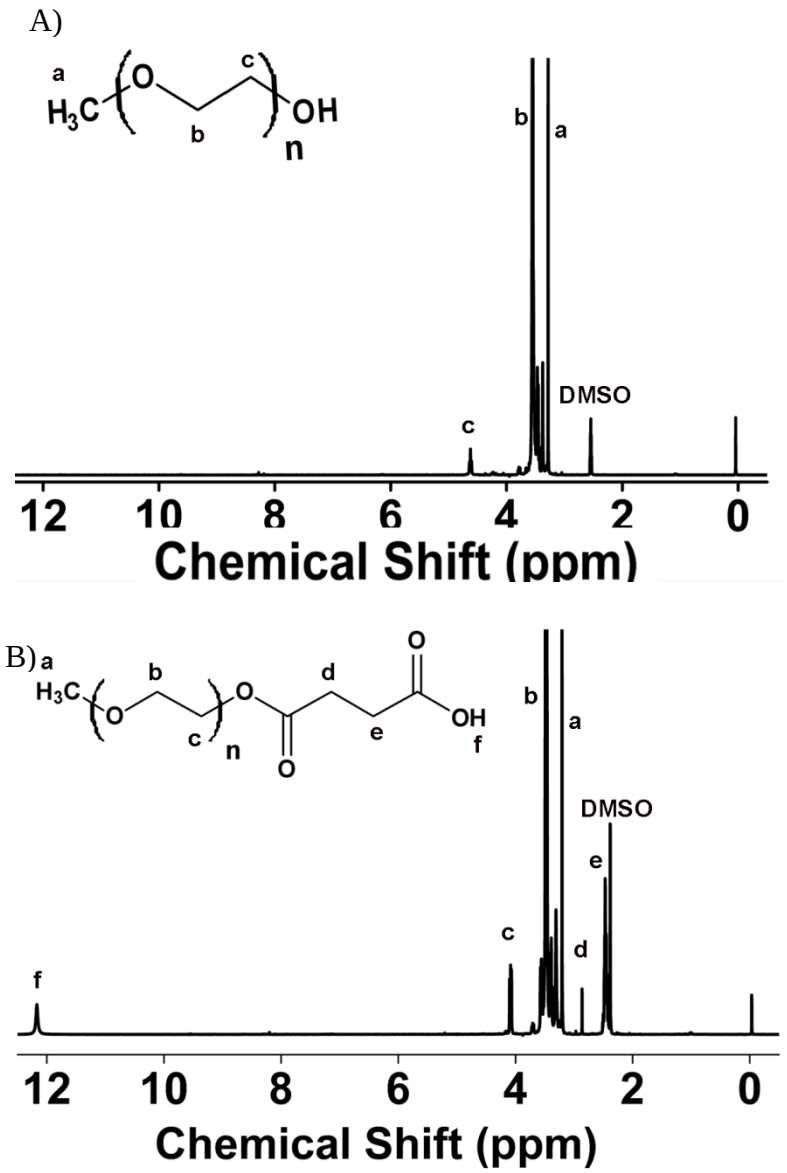

Figure S2. ^{1}H-NMR spectra of A) hydroxyl terminal MPEG; B) carboxylic acid terminal MPEG (MPEG-COOH). The characteristic peaks (a and b) of MPEG located at 3.2 and 3.6 ppm assigned to -C$\underline{H}_3$ and -C$\underline{H}_2$-, respectively, were shown at the same chemical shift for both MPEG and MPEG-COO$\underline{H}$. However, the peak (c) at 4.6 ppm assigned to C$\underline{H}_2$-OH of MPEG shifted to 4.1 ppm due to the conversion of MPEG to MPEG-COOH. Protons (d and e) of methylene groups from succinic acid at 2.8 and 2.2 ppm and protons (f) of COOH groups at 12.1 ppm were observed only on MPEG-COOH confirming the successful termination of MPEG with carboxylic acid.

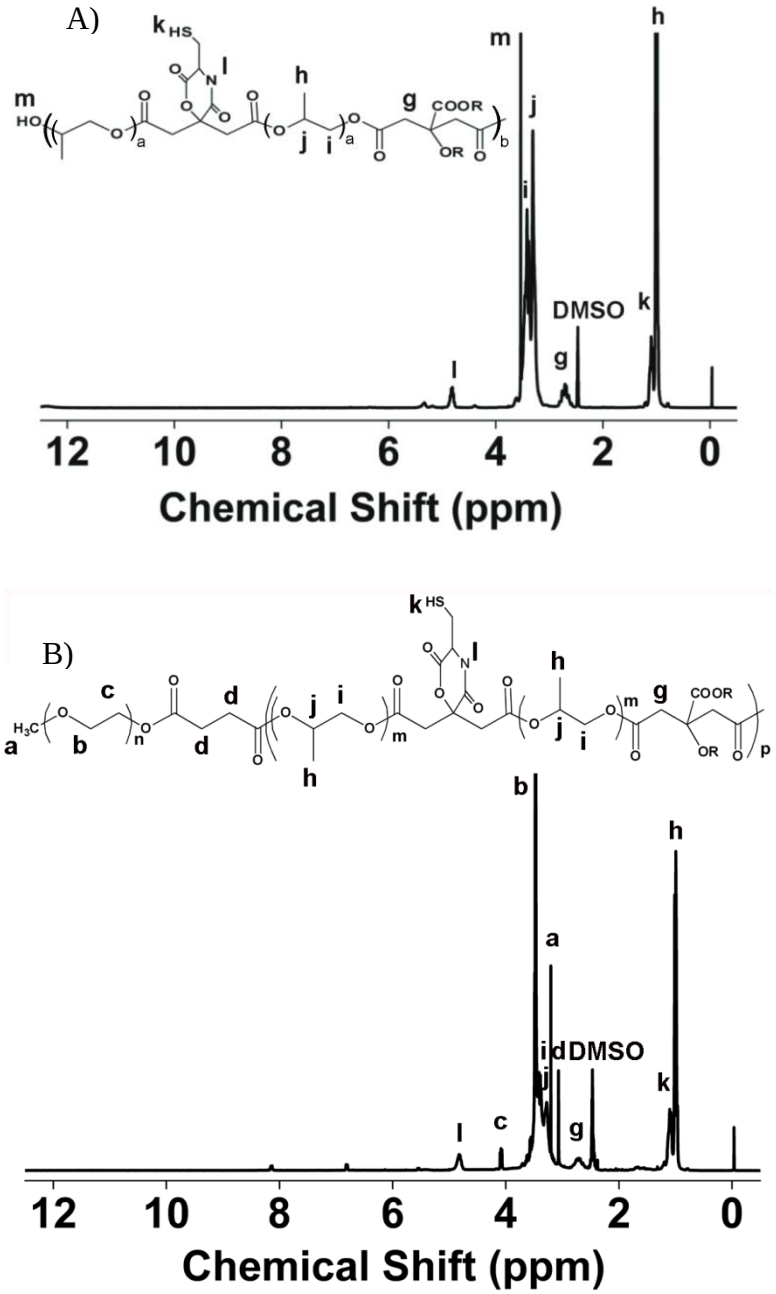

Figure S3. ^{1}H-NMR spectra of A) hydroxyl terminal BPLP; The chemical shifts were in close agreement with the previously reported BPLPs with an additional peak of methyl group from poly(propylene glycol) at 1.1 ppm; B) BPLP conjugated to MPEG-COOH. All characteristic peaks from both hydrophobic and hydrophilic blocks were present in the copolymers absent of a COOH peak located at 12.1 ppm. It should be noted that proton e (**Figure S2B**) located at 2.3 ppm shifted to 3.1 ppm (d in **Figure S3B**) to confirm the successful modification of the neighboring carboxylic groups into ester groups. Furthermore, a significant reduction in the hydroxyl peak was also observed in the FTIR spectrum of amphiphilic block copolymers when compared to the hydrophobic block spectrum alone (**Figure S1**).

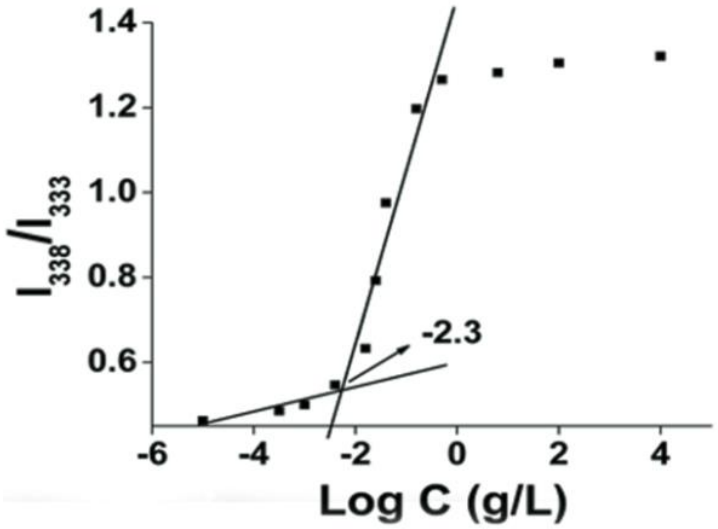

Figure S4. Plot of the intensity ratios I_{338}/I_{333} pyrene vs. log of concentrations (C) of ABPLP-3 in aqueous medium.

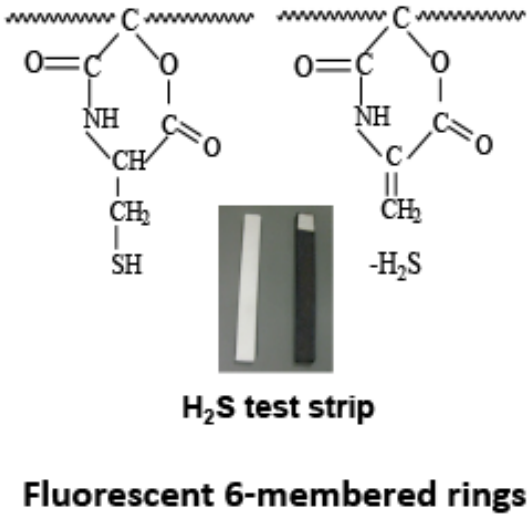

Figure S5. Detection of H_2S elimination using H_2S test strip in ABPLP-Cys synthesis.

A)

Polymer	Drug Loading (%)	Drug Encapsulation(%)
ABPLP-1	21.73	86.91
ABPLP-2	22.36	89.43
ABPLP-3	22.78	91.12
ABPLP-4	20.39	81.57
ABPLP-5	20.6	82.40

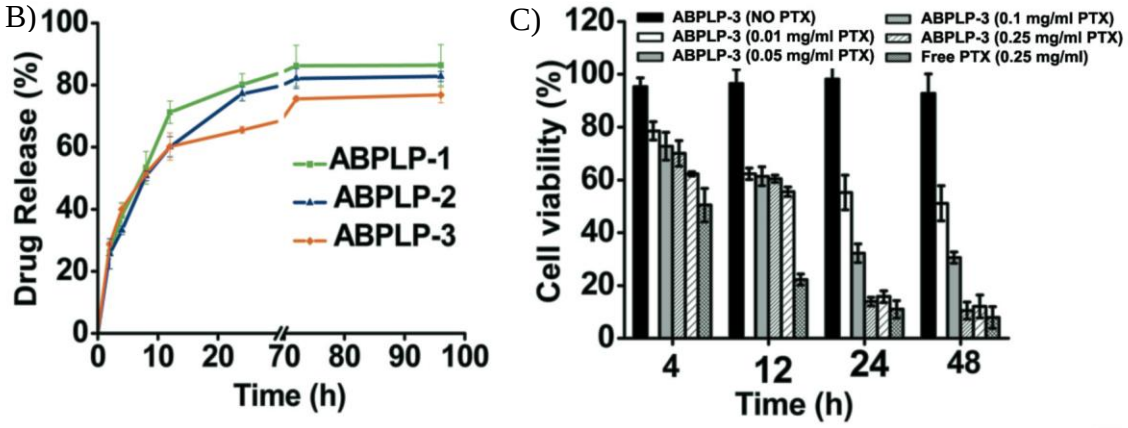

Figure S6. Drug loading and release studies of ABPLP micelles. A) Summary of Drug Loading efficiency of ABPLP Micelles. B) Drug release profile of ABPLP micelles within 96 hours. C) Pharmacological activity of PTX-encapsulated ABPLP over a period of 48 hr against prostate cancer cell lines (PC3) at various dilutions of PTX- loaded ABPLP-3 micelles. Drug free micelles (0.5 mg/ml) and PTX (0.25 mg/ml) were used as negative and positive control respectively. PTX was dissolved in 1% DMSO.